AMERICAN SOCIETY FOR MICROBIOLOGY | Journal of Bacteriology

Functional Interaction between the Cytoplasmic ABC Protein LptB and the Inner Membrane LptC Protein, Components of the Lipopolysaccharide Transport Machinery in *Escherichia coli*

Alessandra M. Martorana,[a] Mattia Benedet,[b]* Elisa A. Maccagni,[a] Paola Sperandeo,[a]* Riccardo Villa,[b]* Gianni Dehò,[b] Alessandra Polissi[a]*

Dipartimento di Biotecnologie e Bioscienze, Università degli Studi di Milano-Bicocca, Milan, Italy[a]; Dipartimento di Bioscienze, Università degli Studi di Milano, Milan, Italy[b]

ABSTRACT

The assembly of lipopolysaccharide (LPS) in the outer leaflet of the outer membrane (OM) requires the transenvelope Lpt (lipopolysaccharide transport) complex, made in *Escherichia coli* of seven essential proteins located in the inner membrane (IM) (LptBCFG), periplasm (LptA), and OM (LptDE). At the IM, LptBFG constitute an unusual ATP binding cassette (ABC) transporter, composed by the transmembrane LptFG proteins and the cytoplasmic LptB ATPase, which is thought to extract LPS from the IM and to provide the energy for its export across the periplasm to the cell surface. LptC is a small IM bitopic protein that binds to LptBFG and recruits LptA via its N- and C-terminal regions, and its role in LPS export is not completely understood. Here, we show that the expression level of *lptB* is a critical factor for suppressing lethality of deletions in the C-terminal region of LptC and the functioning of a hybrid Lpt machinery that carries *Pa*-LptC, the highly divergent LptC orthologue from *Pseudomonas aeruginosa*. We found that LptB overexpression stabilizes C-terminally truncated LptC mutant proteins, thereby allowing the formation of a sufficient amount of stable IM complexes to support growth. Moreover, the LptB level seems also critical for the assembly of IM complexes carrying *Pa*-LptC which is otherwise defective in interactions with the *E. coli* LptFG components. Overall, our data suggest that LptB and LptC functionally interact and support a model whereby LptB plays a key role in the assembly of the Lpt machinery.

IMPORTANCE

The asymmetric outer membrane (OM) of Gram-negative bacteria contains in its outer leaflet an unusual glycolipid, the lipopolysaccharide (LPS). LPS largely contributes to the peculiar permeability barrier properties of the OM that prevent the entry of many antibiotics, thus making Gram-negative pathogens difficult to treat. In *Escherichia coli* the LPS transporter (the Lpt machine) is made of seven essential proteins (LptABCDEFG) that form a transenvelope complex. Here, we show that increased expression of the membrane-associated ABC protein LptB can suppress defects of LptC, which participates in the formation of the periplasmic bridge. This reveals functional interactions between these two components and supports a role of LptB in the assembly of the Lpt machine.

Gram-negative bacteria are surrounded by two lipid bilayers, the inner membrane (IM) and outer membrane (OM), showing distinct composition, structural, and functional properties (1). The two membranes delimit an aqueous compartment, the periplasm, containing a thin peptidoglycan layer. The IM is a symmetric bilayer made of phospholipids, whereas the OM is an asymmetric membrane composed of glycerophospholipids in the inner leaflet and lipopolysaccharide (LPS) in the outer leaflet (1). LPS is a complex glycolipid assembled at the outer leaflet of the OM, where it forms a permeability barrier that prevents entry of many hydrophobic toxic compounds, including antibiotics (2). In *Escherichia coli*, LPS export to the cell surface is performed by a transenvelope complex of seven essential Lpt proteins (LptABCDEFG) spanning across the four-cell compartment from cytoplasm to OM (3–7). At the IM, $LptB_2FG$ constitute an ATP binding cassette (ABC) transporter that provides energy to the LPS transport system (8–10). LptC is a bitopic IM protein that associates with the IM $LptB_2FG$ transporter (8). The β-barrel LptD protein and the LptE lipoprotein constitute the OM translocon, characterized by a unique plug and barrel architecture, responsible for the final stages of LPS assembly at the cell surface (11–14). LptA is the key periplasmic component of the machinery that connects the IM and OM complexes (5, 15, 16).

The crystal structures of five components of the Lpt machinery, LptC from *E. coli* (17), LptA from *E. coli* and *Pseudomonas aeruginosa* (18, 19), the LptD-LptE complex from *Shigella flexneri* and *Salmonella enterica* serovar Typhimurium (12, 20), and the cytoplasmic ABC protein LptB from *E. coli* (10, 21), have been solved. Interestingly, LptA, the periplasmic region of LptC, and

Received 21 April 2016 **Accepted** 24 May 2016

Accepted manuscript posted online 31 May 2016

Citation Martorana AM, Benedet M, Maccagni EA, Sperandeo P, Villa R, Dehò G, Polissi A. 2016. Functional interaction between the cytoplasmic ABC protein LptB and the inner membrane LptC protein, components of the lipopolysaccharide transport machinery in *Escherichia coli*. J Bacteriol 198:2192–2203. doi:10.1128/JB.00329-16.

Editor: V. J. DiRita, Michigan State University

Address correspondence to Alessandra Polissi, alessandra.polissi@unimib.it.

* Present address: Mattia Benedet, Center for Integrative Biology, Università degli Studi di Trento, Trento, Italy; Paola Sperandeo and Alessandra Polissi, Dipartimento di Scienze Farmacologiche e Biomolecolari, Università degli Studi di Milano, Milan, Italy; Riccardo Villa, Frau Pharma, Agrate Brianza (MB), Italy.

Supplemental material for this article may be found at http://dx.doi.org/10.1128/JB.00329-16.

the periplasmic N-terminal region of LptD, despite a lack of sequence similarity, share a very similar β-jellyroll fold, made of the juxtaposition of a variable number of antiparallel β strands. Such a β-jellyroll fold (the Lpt fold) appears to be a key element in driving the assembly of the Lpt machinery. In fact, through these structurally homologous domains, the C terminus of LptC interacts with the N terminus of LptA, and the C terminus of LptA interacts with the N-terminal periplasmic domain of LptD, thus forming a protein bridge that connects the IM and the OM (12, 16, 20, 22).

The assembly of the transenvelope bridge appears to be finely regulated to prevent LPS mistargeting. Proper interaction of LptC with $LptB_2FG$ is necessary for LptA recruitment (22). Interaction of the N-terminal domain of LptD with LptA requires the correct maturation of the LptDE complex that in turns depends on nonconsecutive disulfide bond formation in LptD (16); LptE and the chaperone/protease BepA have been implicated in this process (23). Based on *in vivo* photo-cross-linking experiments, LPS molecules appear to cross the periplasm inside the β jellyroll of LptC and LptA (9). ATP hydrolysis by LptB, the cytoplasmic ATPase of the $LptB_2FG$ transporter, is required for LPS extraction from the IM and its transfer to LptA via LptC. Energy does not seem to be required for the assembly of the transenvelope bridge (9). Nevertheless, LptB also plays a role in the IM LptCFG subcomplex assembly, as shown by *lptB* mutants defective in assembly but proficient in the ATPase activity (10).

The molecular role of LptC in LPS transport is still elusive. LptC does not seem to be a functional component of the IM ABC transporter, as its association with the $LptB_2FG$ complex does not affect its ATPase activity (8); on the other hand, it appears relevant for proper IM complex assembly (22). Mutational analyses suggest that the interaction of LptC with the IM $LptB_2FG$ complex is mediated by the N-terminal region of the β jellyroll, whereas its transmembrane domain appears to be dispensable, as a periplasmic soluble version of LptC and a LptC chimera carrying a heterologous transmembrane segment is functional and proficient in Lpt complex assembly (22).

To gain further insights into the role of LptC in the LPS export pathway, we dissected *E. coli* LptC (*Ec*-LptC) functional domains by analyzing the phenotype of *E. coli lptC* mutants and the properties of LptC from *P. aeruginosa* (*Pa*-LptC) and *Ec*-/*Pa*-LptC chimeras in *E. coli*. We show that *lptB* ectopic expression suppresses the lethality of C-terminal deletion of LptC and allows the functioning of hybrid Lpt machinery that carries the highly divergent LptC orthologue from *P. aeruginosa*.

MATERIALS AND METHODS

Bacterial strains, plasmids, and growth conditions. *E. coli* bacterial strains used in this study are listed in Table 1. Left and right junctions of Tn*SS2* inserted in the ST-190 mutants were sequenced upon amplification of the two regions with oligonucleotide pairs AP23-FG1676 and FG690-AP179, respectively. *P. aeruginosa* PAO1 (25) was used as a source of *P. aeruginosa* DNA. Plasmids are listed in Table 2 with a brief outline of their construction by standard cloning techniques and, where indicated, three-step PCR (26). Chimeric *lptC* alleles and proteins are designated by three letters following the gene/protein name indicating sequentially the source, from either *E. coli* (C) or *P. aeruginosa* (P), of regions 1, 2, and 3, as defined in Fig. 1; -H indicates the His_6 tag at the C terminus. Oligonucleotides used as primers for plasmid engineering and/or sequencing are listed in Table S1 in the supplemental material. All cloned PCR products were verified by DNA sequencing. Bacteria were grown in LD medium (27). When required, 0.2% (wt/vol) L-arabinose (as an inducer of the *araBp* promoter), 0.1 mM IPTG (isopropyl-β-D-thiogalactopyranoside), 25 μg/ml chloramphenicol, and 100 μg/ml ampicillin were added. Solid media were prepared as described above with 1% (wt/vol) agar.

TABLE 1 *E. coli* strains

Strain	Description[a]	Reference
AM604	MC4100 Ara^+	3
AMM04	AM604 *lptD*-SPA::*kan*	22
DH5α	Δ(*argF-lac*)*169* ϕ80d*lacZ58*(M15) *glnV44*(AS) λ^- *rfbD1 gyrA96 recA1 endA1 spoT1 thi-1 hsdR17*	40
DH10B	*araD139* Δ(*ara-leu*)*7697* Δ*lacX74 galU galK rpsL deoR* ϕ80d*lacZ*ΔM15 *endAI nupG recAl mcrA* Δ(*mrr hsdRMS mcrBC*)	41
FL905	AM604 Φ(*kan araC araBp-lptC*)	5
MC4100	F^- *araD139* Δ(*argF-lac*)*U169 rpsL150* (Str^r) *relA1 flbB5301 deoC1 ptsF25 rbsR*	42
MG1655	K-12 F^- λ^- *ilvG rfb-50 rph-1*	43
ST-190	Δ(*ara-leu*) *araD* Δ*lacX74 galE galK phoA20 thi-1 rpsE rpoB* (Rif^r) *argE*(Am) *recA1* λ^R *lptC*::Tn*SS2*	24

[a] AS, amber suppressor.

Identification of motifs in LptC. The MM algorithm (28) from the MEME suite (29) (http://meme.nbcr.net/meme/tools/meme) was applied to analyze protein sequences for the occurrence of amino acid motifs. A motif is a sequence pattern that occurs repeatedly in a group of evolutionarily related proteins. The MM algorithm is capable of discovering different motifs with different number occurrences in a single data set. The algorithm estimates how many times each motif occurs in each sequence in the data set, ordering the motifs found with a statistical significance. Default settings have been applied to perform an *ab initio* motif discovery procedure to search for no more than 3 motifs on amino acid sequences of LptC homologues from a set of 13 representative taxa within *Gammaproteobacteria* (see Fig. S1 in the supplemental material). Motifs 1, 2, and 3 were numbered in an order based on statistical significance (Fig. 1; see also Fig. S1A). To correlate motif divergence and genetic distance among LptC homologues, a multialignment was performed with Multalin software, available online (http://multalin.toulouse.inra.fr/multalin/) (30), applying a modified blosum62 (blocks substitution) matrix for the amino acid substitution in proteins alignment (31), setting gap weight and gap length weight as 1 and 2, respectively. An LptC dendrogram was finally depicted, expressing the phylogenetic distance as a Dayhoff-Eck or point-accepted mutation (PAM), setting 20 PAMs as the minimal distance between sequences (see Fig. S1B). The overall phylogeny of the representative taxa selected among *Gammaproteobacteria* was compared to the LptC dendrogram, using the phylogenic tree proposed by Williams et al. (32) (see Fig. S1B).

The three-dimensional structures of *Pa*-LptC (PA4459) and *Ec*-$LptC^{\Delta 139\text{-}191}$ (*Ec*-LptC with amino acids 139 to 191 deleted) were predicted using the online platform I-TASSER (iterative threading assembly refinement [http://zhanglab.ccmb.med.umich.edu/I-TASSER/]) (33). The computational models were obtained by threading, recognizing the *E. coli* LptC X-ray crystal structure (PDB no. 3MY2) (17) as the best template. Graphical modeling and superimposition were performed by Pymol (Pymol molecular graphics system, version 1.8; Schrödinger, LLC; www.pymol.org).

Complementation assay. FL905 (*araBp-lptC*) carrying plasmids expressing different *Ec-lptC* or *Pa-lptC* alleles or chimeras, alone or in combination with *Ec-lptA*, *lptB*, or *lptAB* (see Table 2), were grown at 37°C in LD containing chloramphenicol (25 μg/ml) and arabinose (0.2%) for 18 h. Serial 10-fold dilutions in microtiter wells of the cultures were then replica plated on agar plates containing 25 μg/ml chloramphenicol, with or without 0.2% arabinose, and incubated overnight at 37°C.

TABLE 2 Plasmids

Plasmid	Parental plasmid/ replicon	Relevant characteristic(s)	Construction/origin[a] or reference
pGS100	pGZ11EH	*ptac*-TIR *cat ori*V_{ColD}	44
pGS103	pGS100	*ptac-lptC cat*	44
pGS104	pGS100	*ptac-lptCAB cat ori*V_{ColD}	44
pGS103G153R	pGS100	*ptac-lptC*^{G153R} *cat*	15
pGS108	pGS100	*ptac-lptC-H cat*	44
pGS111	pGS100	*ptac-Pa-lptC cat*	*Pa-lptC* was PCR amplified with AP175 and AP176 primers from *P. aeruginosa* PAO1 genomic DNA and cloned into EcoRI-HindIII sites of pGS100
pGS200	pGS100	*ptac-Pa-lptC-H cat*	*Pa-lptC* was PCR amplified with AP175 and AP237 primers from pGS111 and cloned into EcoRI-HindIII sites of pGS100
pGS201	pGS100	*ptac-lptC-CPP cat*	*lptC-CPP* was obtained by three step PCR with AP91, AP192, AP92, AP191 primers from pGS103 and pGS111 as templates and cloned into EcoRI-HindIII sites of pGS100
pGS201H	pGS100	*ptac-lptC-CPP-H cat*	*lptC-CPP-H* was PCR amplified with AP91 and AP237 primers from pGS201 and cloned into EcoRI-HindIII sites of pGS100
pGS202	pGS100	*ptac-lptC-PCC cat*	*lptC-PCC* was obtained by three-step PCR with AP91, AP195, AP92, AP196 primers from pGS103 and pGS111 as templates and cloned into EcoRI-HindIII sites of pGS100
pGS202H	pGS100	*ptac-lptC-PCC-H cat*	*lptC-PCC-H* was PCR amplified with AP91 and AP63 primers from pGS202 and cloned into EcoRI-HindIII sites of pGS100
pGS203	pGS100	*ptac-lptC-CPC cat*	*lptC-CPC* was obtained by three-step PCR with AP91, AP194, AP91, and AP193 primers from pGS201 and pGS103 as templates and cloned into EcoRI-HindIII sites of pGS100
pGS203H	pGS100	*ptac-lptC-CPC-H cat*	*lptC-CPC-H* was PCR amplified with AP91 and AP63 primers from pGS203 and cloned into EcoRI-HindIII sites of pGS100
pGS204	pGS100	*ptac-lptC-PCP cat*	*lptC-PCP* was obtained by three-step PCR with AP91, AP198, AP92, and AP197 primers from pGS202 and pGS111 as templates and cloned into EcoRI-HindIII sites of pGS100
pGS204H	pGS100	*ptac-lptC-PCP-H cat*	*lptC-PCP-H* was PCR amplified with AP91 and AP237 primers from pGS204 and cloned into EcoRI-HindIII sites of pGS100
pGS206	pGS100	*ptac-lptC-CCP cat*	*lptC-CCP* was obtained by three-step PCR with AP91, AP198, AP92, and AP197 primers from pGS103 and pGS111 as templates and cloned into EcoRI-HindIII sites of pGS100
pGS206H	pGS100	*ptac-lptC-CCP-H cat*	*lptC-CCP-H* was PCR amplified with AP91 and AP237 primers from pGS206 and cloned into EcoRI-HindIII sites of pGS100
pGS207	pGS100	*ptac-lptC-PPC cat*	*lptC-PPC* was obtained by three-step PCR with AP91, AP194, AP92, and AP193 primers from pGS111 and pGS103 as templates and cloned into EcoRI-HindIII sites of pGS100
pGS207H	pGS100	*ptac-lptC-PPC-H cat*	*lptC-PPC-H* was PCR amplified with AP91 and AP63 primers from pGS207 and cloned into EcoRI-HindIII sites of pGS100
pGS208	pGS100	*ptac-lptC-CC*Δ *cat*	*lptC-PCP* was PCR amplified with AP91 and AP63 primers from pGS103 and cloned into EcoRI-HindIII sites of pGS100
pGS208H	pGS100	*ptac-lptC- CC*Δ*-H cat*	*lptC-PCP-H* was PCR amplified with AP91 and AP361 primers from pGS103 and cloned into EcoRI-HindIII sites of pGS100
pGS321	pGS100	*ptac-lptA cat*	*lptA* was PCR amplified with AP55 and FG2723 primers from pGS104 and cloned into EcoRI-XbaI sites of pGS100
pGS401	pGS100	*ptac*-SD1-EcoRI-XbaI-SD2-SalI-HindIII *cat*	19
pGS402	pGS401	*ptac-lptC cat*	19
pGS403	pGS401	*ptac-Pa-lptC cat*	*Pa-lptC* was PCR amplified with AP175 and AP176 primers from *P. aeruginosa* PAO1 DNA and cloned into EcoRI-XbaI sites of pGS401 downstream of SD1
pGS404	pGS402	*ptac-lptC-lptA cat*	19
pGS407	pGS403	*ptac-Pa-lptC-lptA cat*	*Ec-lptA* was PCR amplified with FG2935 and FG2936 primers from MG1655 DNA and cloned into SalI-HindIII sites of pGS403 downstream of SD2
pGS408	pGS401	*ptac-lptC190N cat*	*lptC190N* was PCR amplified with FG2978 and FG2979 primers from ST-190 genomic DNA and cloned into EcoRI-XbaI sites of pGS401
pGS411	pGS407	*ptac-lptC190N-lptA cat*	*lptC190N* was PCR amplified with FG2978 and FG2979 primers from ST-190 genomic DNA and cloned into EcoRI-XbaI sites of pGS407
pGS412	pGS407	*ptac-lptC*^{G153R}*-lptA cat*	*lptC*G153R was obtained by EcoRI-XbaI digestion of pGS103G153R and cloned into EcoRI-XbaI sites of pGS407

(Continued on following page)

TABLE 2 (Continued)

Plasmid	Parental plasmid/ replicon	Relevant characteristic(s)	Construction/origin[a] or reference
pGS413	pGS412	*ptac-lptC*^{G153R}*-lptAB cat*	*Ec-lptAB* was PCR amplified with FG2935 and FG3058 primers from MG1655 DNA and cloned into SalI-HindIII sites of pGS412
pGS414	pGS408	*ptac-lptC190N-lptAB cat*	*Ec-lptAB* was PCR amplified with FG2935 and FG3058 primers from MG1655 DNA and cloned into SalI-HindIII sites of pGS408
pGS415	pGS402	*ptac-lptC-lptAB cat*	*Ec-lptAB* was PCR amplified with FG2935 and FG3058 primers from MG1655 DNA and cloned into SalI-HindIII sites of pGS402
pGS416	pGS401	*ptac*-void-*lptAB cat*	19
pGS417	pGS401	*ptac-lptC*$^{\Delta 139\text{-}191}$ *cat*	*Ec-lptC*$_{1\text{-}138}$ was PCR amplified with FG2978 and FG3088 primers from pGS402 and cloned into EcoRI-XbaI sites of pGS401
pGS418	pGS407	*ptac-lptC*$^{\Delta 139\text{-}191}$*-lptA cat*	*Ec-lptC*$_{1\text{-}138}$ was PCR amplified with FG2978 and FG3088 primers from pGS402 and cloned into EcoRI-XbaI sites of pGS407
pGS419	pGS416	*ptac-lptC*$^{\Delta 139\text{-}191}$*-lptAB cat*	*Ec-lptC*$_{1\text{-}138}$ was PCR amplified with FG2978 and FG3088 primers from pGS402 and cloned into EcoRI-XbaI sites of pGS416
pGS428	pGS401	*ptac*-void-*lptB cat*	19
pGS429	pGS402	*ptac-lptC-lptB cat*	*Ec-lptB* was obtained by SalI-HindIII digestion of pGS428 and cloned into SalI-HindIII sites of pGS402
pGS429-LptB^{E163Q}	pGS429	*ptac-lptC-lptB*^{E163Q} *cat*	E163Q substitution was obtained by site-directed mutagenesis with AP471 and AP472 primers from pGS429 as the template
pGS429-LptB^{F90A}	pGS429	*ptac-lptC-lptB*^{F90A} *cat*	F90A substitution was obtained by site-directed mutagenesis with AP467 and AP468 primers from pGS429 as the template
pGS429-LptB^{F90Y}	pGS429	*ptac-lptC-lptB*^{F90Y} *cat*	F90Y substitution was obtained by site-directed mutagenesis with AP469 and AP470 primers from pGS429 as the template
pGS430	pGS408	*ptac-lptC190N-lptB cat*	*Ec-lptB* was obtained by SalI-HindIII digestion of pGS428 and cloned into SalI-HindIII sites of pGS408
pGS431	pGS417	*ptac-lptC*$^{\Delta 139\text{-}191}$*-lptB cat*	*Ec-lptB* was obtained by SalI-HindIII digestion of pGS428 and cloned into SalI-HindIII sites of pGS417
pGS431-LptB^{E163Q}	pGS431	*ptac-lptC*$^{\Delta 139\text{-}191}$*-lptB*^{E163Q} *cat*	E163Q substitution was obtained by site-directed mutagenesis with AP471 and AP472 primers from pGS431 as the template
pGS431-LptB^{F90A}	pGS431	*ptac-lptC*$^{\Delta 139\text{-}191}$*-lptB*^{F90A} *cat*	F90A substitution was obtained by site-directed mutagenesis with AP467 and AP468 primers from pGS431 as the template
pGS431-LptB^{F90Y}	pGS431	*ptac-lptC*$^{\Delta 139\text{-}191}$*-lptB*^{F90Y} *cat*	F90Y substitution was obtained by site-directed mutagenesis with AP469 and AP470 primers from pGS431 as the template
pGS434	pGS412	*ptac-lptC*^{G153R}*-lptB cat*	*Ec-lptB* was obtained by SalI-HindIII digestion of pGS428 and cloned into SalI-HindIII sites of pGS412
pGS439	pGS401	*ptac-lptC*^{G153R} *cat*	*lptC*^{G153R} was obtained by EcoRI-XbaI digestion of pGS412 and cloned into EcoRI-XbaI sites of pGS401
pGS440	pGS401	*ptac*-void-*lptA cat*	*lptA* was obtained by SalI-HindIII digestion of pGS404 and cloned into SalI-HindIII sites of pGS401
pGS448	pGS416	*ptac-Pa-lptC-lptAB cat*	*Pa-lptC* was obtained by EcoRI-XbaI digestion of pGS407 and cloned into EcoRI-XbaI sites of pGS416
pGS456	pGS428	*ptac-Pa-lptC-lptB cat*	*Pa-lptC* was PCR amplified with AP175 and AP176 primers from *P. aeruginosa* PAO1 genomic DNA and cloned into EcoRI-XbaI sites of pGS428

[a] *Ec-lptC*$_{1\text{-}138}$, *Ec-lptC* encoding amino acids 1 to 138.

Determination of LptA, LptC, LptB, and LptE levels. LptA, LptC, LptB, and LptE levels were assessed in FL905 coexpressing wild-type or truncated LptC proteins with LptA or LptB or LptAB by Western blotting using polyclonal antibodies raised in mouse or rabbit against peptides (LptA and LptB) or whole proteins (LptE, LptC). Bacterial cultures grown up to an optical density at 600 nm (OD_{600}) of 0.2 at 37°C in LD supplemented with 0.2% arabinose and 25 μg/ml of chloramphenicol were harvested by centrifugation, washed in LD, and diluted 500-fold in fresh media with or without 0.2% arabinose and with 25 μg/ml chloramphenicol. Growth was monitored by measuring the OD_{600}. Samples for protein analysis were collected 240 min after the shift to nonpermissive conditions and centrifuged (16,000 × *g*, 5 min), and pellets were resuspended in a volume (in ml) of SDS sample buffer equal to 1/24 of the total OD of the sample. Samples were boiled for 10 min, and equal volumes (20 μl) were analyzed by 12.5% polyacrylamide-SDS gel electrophoresis. Proteins were transferred onto nitrocellulose membranes (GE Healthcare), and Western blot analysis was performed as previously described (4). Polyclonal sera raised against LptC and LptA (GenScript Corporation) were used as the primary antibody at a dilution of 1:500, whereas polyclonal sera against LptE and LptB (kindly provided by D. Khane and N. Ruiz, respectively) were used at a dilution of 1:5,000 and 1:1,000, respectively. Polyclonal serum raised against the S1 protein (kindly provided by F. Briani) was used at a dilution of 1:10,000. As secondary antibodies, anti-goat, anti-rabbit, and anti-mouse immunoglobulins (Li-Cor) were used at a dilution of 1:15,000.

Affinity purification of membrane Lpt complexes. AMM04 cells harboring plasmids expressing His-tagged *Ec*-LptC, *Pa*-LptC, and LptC chimeras were subjected to affinity purification as previously described (7), with few modifications. The cells were lysed by a single cycle through a cell disrupter (One Shot Model; Constant Systems, Ltd) at a pressure of 22,000 lb/in^2, and membranes were collected by ultracentrifugation of the supernatant at 100,000 × *g* for 1 h. The membranes were extracted at 4°C for 30 min with 5 ml of 50 mM Tris-HCl (pH 7.4), 10% glycerol, 1% dodecyl β-D-maltoside (Anatrace), and 5 mM $MgCl_2$. The mixture was centri-

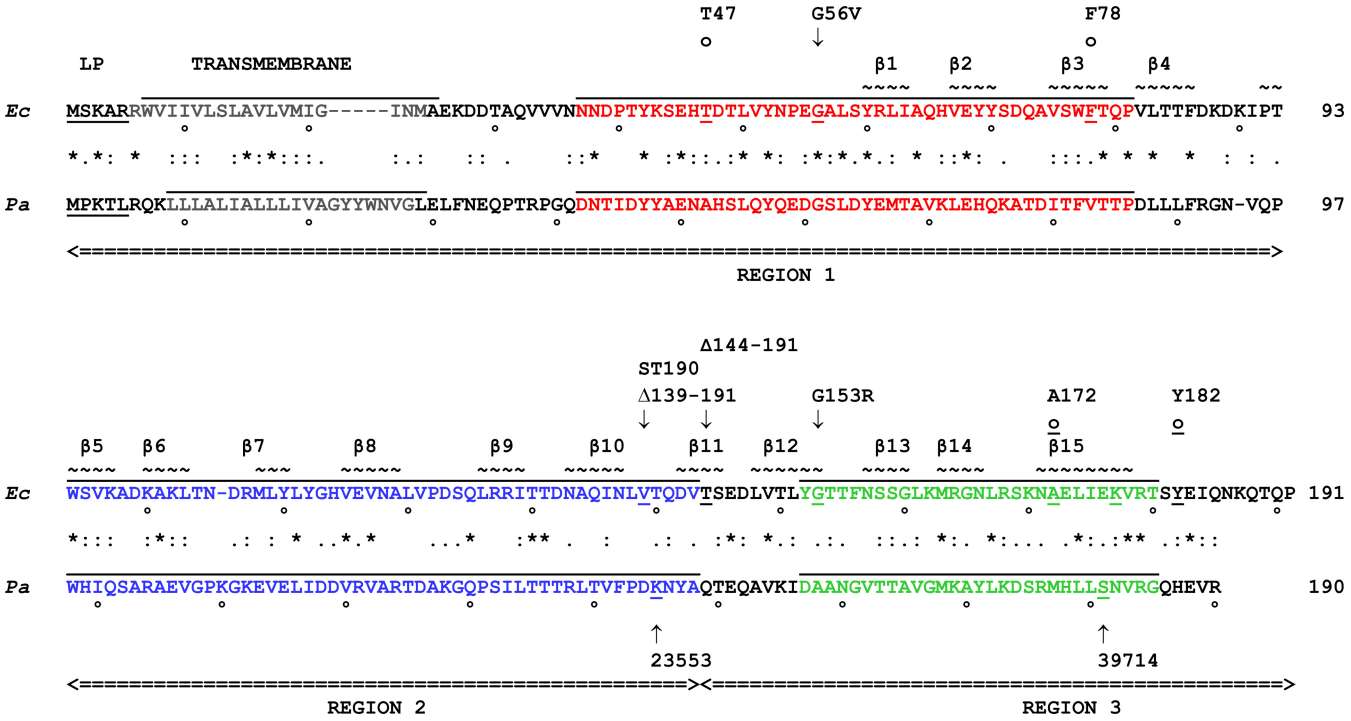

FIG 1 Comparison of *E. coli* and *P. aeruginosa* LptC amino acid sequences and structures. Amino acid sequence alignment of LptC from *E. coli* (*Ec*-LptC) and *P. aeruginosa* (*Pa*-LptC). Amino acid identity (asterisk) and similarity (colon and period) are labeled. Leader peptide (LP) and transmembrane regions are indicated. Regions 1, 2, and 3 swapped in chimera constructions are delimited by arrowheads at the end of double underlining. Sequences corresponding to the MEME motifs are overlined and color coded as follows: blue, motif 1 (residues 94 to 143); red, motif 2 (residues 37 to 81); green, motif 3 (residues 152 to 180). Relevant LptC mutations are indicated above and below the *E. coli* and *P. aeruginosa* sequences, respectively. Arrows indicate the mutated amino acid (for point mutations), the first deleted amino acid (for deletions), and the first amino acid at the right of the inserted transposon. ST-190, transposon insertion in ST-190 (24); 23553 and 39714 indicate two transposon insertions in *Pa-lptC* (http://ausubellab.mgh.harvard.edu). o and o indicate amino acids photo-cross-linked to LPS and LptA, respectively (9, 16). Tilde marks indicate amino acids in β strands, progressively numbered (17).

fuged again at 100,000 × *g* for 1 h, and insoluble material was discarded. The supernatant was incubated with 0.5 ml Talon resin suspension for 30 min at 4°C, and the mixture was then loaded onto a column. The column was washed with 10 ml of 50 mM Tris-HCl (pH 7.4), 10% glycerol, 0.05% dodecyl maltoside, and 5 mM imidazole, and eluted with 5 ml of 50 mM Tris-HCl (pH 7.4), 10% glycerol, 0.05% dodecyl maltoside, and 200 mM imidazole. The eluate was concentrated using an ultrafiltration device (Amicon Ultra, Millipore) by centrifugation at 5,000 × *g* to a final volume of 50 μl. Samples were mixed with 2× loading buffer, boiled, and separated on SDS-PAGE gel, electroblotted, and immunodetected using anti-His monoclonal antibodies (1:3,000) (Sigma-Aldrich) to detect wild-type *Ec*- and *Pa*-LptC-H and LptC-H chimeras and anti-LptA (1:2,000), LptB (1:1,000), LptD (1:500), and LptF (1:2,000), as previously described (22).

RESULTS

Complementation of *E. coli lptC* conditional mutant by *lptC* from *P. aeruginosa*. A BLAST (http://blast.ncbi.nlm.nih.gov/Blast.cgi) search using the amino acid sequence of LptC from *Escherichia coli* K-12 (Uniprot accession no. P0ADV9) as a query against the translated *P. aeruginosa* strain PAO1 genomic sequence (accession no. NC_002516.2) (http://www.pseudomonas.com/) identified a conserved putative protein of 190 amino acids with ~20% sequence identity (Fig. 1) encoded by PA4459. This putative gene is located upstream of *lptH* (PA4460) and experimentally is demonstrated as the *Pseudomonas* homologue of *lptA* (19). Despite the low sequence similarity, the Pfam algorithm (34) predicts for the PA4459-encoded protein the same β-jellyroll domain found in *Ec*-LptC (17) (see Fig. S2 in the supplemental material). Overall, these data strongly suggest that PA4459 is the homologue of *Ec-lptC* and is herewith designated *Pa-lptC*.

We then tested whether *Pa-lptC* could complement the *E. coli lptC* conditional expression mutant under nonpermissive conditions. The reference *lptC* complementation test was performed in FL905, an *E. coli araBp-lptC* arabinose-dependent mutant (5), in which the complementing *lptC* allele is ectopically expressed at the basal level from the *ptac* promoter of the pGS100 vector. It should be noted that the level of *lptC* expressed from the plasmid is higher than that expressed from a native chromosomal promoter(s) (15). Moreover, under nonpermissive conditions (no chromosomal *lptC* expression in the absence of arabinose), expression of the downstream *lptAB* genes is driven by the minor promoters *lptAp1* and *lptAp2* (σ^E- and σ^D-dependent, respectively) located within the *lptC* coding region (35). FL905 was thus transformed with plasmid pGS200, which expresses *Pa-lptC* from the *ptac* promoter. As shown in Fig. 2, *Pa-lptC*, unlike the *Ec-lptC* control, did not complement FL905 for growth in the nonpermissive (no arabinose) conditions.

Construction and expression of *E. coli-P. aeruginosa* LptC chimeras. Sequence alignments among LptC homologues in a subset of representative taxa within *Gammaproteobacteria* using the MEME suite software (29) were performed to identify conserved sequence motifs in the LptC family of proteins. LptC multiple alignments recognized three sequence motifs in all representative LptC homologues taken into consideration, with the

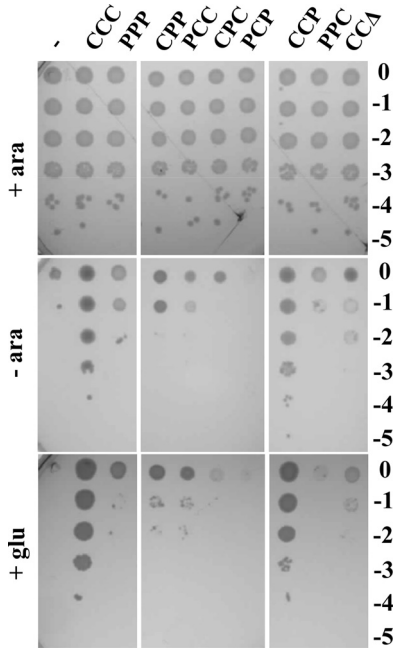

FIG 2 Complementation test of LptC depletion mutants with different *E. coli* and *P. aeruginosa* wild-type or chimeric LptC constructs. Cultures of FL905 (*araBp-lptC*) strains freshly transformed with pGS100 derivatives expressing *Ec*-LptC (pGS103, CCC), *Pa*-LptC (pGS111, PPP), LptC chimeras (pGS201, CPP; pGS202, PCC; pGS203, CPC; pGS204, PCP; pGS206, CCP; pGS207, PPC), or a truncated *Ec*-LptC protein missing region 3 (pGS208, CCΔ) and grown in LD-chloramphenicol-arabinose were serially diluted 1:10 in microtiter wells and replica plated in agar plates with (+ ara) or without (− ara) arabinose or with glucose (+ glu) to fully repress the *araBp* promoter. The log of the serial dilutions is indicated on the right of the panel.

exception of those from *P. aeruginosa* and *Legionella pneumophila* (see Fig. S1A in the supplemental material). This observation is in agreement with the phylogenetic distances of such taxa (32) (see Fig. S1B). According to MEME analysis, motif 3 (which spans amino acids 152 to 180) is the least conserved across species, whereas motif 1 (amino acids 94 to 143), which is the most conserved in other bacteria, was recognized in neither *L. pneumophila* LptC nor *P. aeruginosa* LptC. As shown in Fig. 1 and in Fig. S1A in the supplemental material, motif 2 is located in the N-terminal region of LptC (region 1) and the most conserved motif, motif 1, lies in the central portion of the protein (region 2), whereas motif 3 is located at the C-terminal end of LptC (region 3).

To assess whether the lack of complementation by *Pa*-LptC could be imputed to any of the three regions, we swapped these three different regions of *Ec*- and *Pa*-LptC in all possible combinations, cloned the entire set of chimeric constructs in the pGS100 plasmid vector under the control of the *ptac* promoter, and tested the *lptC* chimeras by the reference *lptC* complementation assay. Only the chimeric protein that carries *E. coli* regions 1 and 2 and *P. aeruginosa* region 3 (CCP chimera) was able to support the growth of the *araBp-lptC* conditional mutant (Fig. 2).

Lpt complex assembly by LptC chimeras. LptC is a component of the Lpt machinery and interacts with both the IM protein complex LptBFG and the periplasmic component LptA (8, 15, 22). The assembly of the Lpt machinery is a highly coordinated multistep process, as interaction of LptC with the IM complex LptBFG is required to recruit LptA and the OM complex LptDE (22). We therefore investigated by affinity purification experiments on the purified membrane fraction, as previously described (7, 22), whether the LptC chimeras are able to properly interact with the IM Lpt components and then to assemble the Lpt export machinery. C-terminal His-tagged *Ec*-LptC, *Pa*-LptC, and LptC chimeras expressed from the pGS100 vector in AM604 strain were used as baits in pulldown experiments. All His-tagged constructs behaved as the untagged counterparts for the ability, or lack thereof, to complement the *araBp-lptC* conditional mutant for growth (see Fig. S3 in the supplemental material). Total membranes collected from cells expressing C-terminally His-tagged *Ec*-, *Pa*-, or chimeric LptC proteins were solubilized, and the Lpt complexes with the different LptC baits were affinity purified. Samples were then processed by immunoblotting with a panel of specific antibodies. First, we assessed the ability of *Pa*-LptC and the chimeric proteins to recruit the IM complex LptBFG by revealing the presence of LptF with anti-LptF antibodies. As judged by the copurification profile shown in Fig. 3A it appears that only the complementing CCP chimera binds to the inner membrane component LptF at a level comparable to that of *Ec*-LptC. On the contrary, *Pa*-LptC and the noncomplementing chimeras fail to assemble the IM complex, as they are all unable to interact with LptF (Fig. 3A). Indeed, based on the copurification profile of LptA, LptD, and LptE shown in Fig. 3B, the CCP chimera but not *Pa*-LptC is able to recruit LptA and the LptDE complex and thus to assemble the whole Lpt machine.

These results implicate *E. coli* LptC regions 1 and 2 in the interaction with the $LptB_2FG$ complex. Moreover, the fact that a xenogeneic region 3 allows the recruitment of Ec-LptA and therefore the assembly of the Lpt machine suggests that either LptC region 3 is not relevant for LptC functionality or that the Lpt fold, rather than a specific amino acid sequence, is required to fulfill LptC function(s).

LptC region 3 may be dispensable. Previous data (15, 16, 22) implicated the C-terminal region of *Ec*-LptC (which encompasses region 3) (Fig. 1) in binding with LptA. In particular, the *Ec*-LptC residues A172 and Y182 are thought to interact with LptA (16), whereas the G153R amino acid change in *Ec*-LptC (encoded by *Ec-lptC*^{G153R}) not only is lethal but also impairs LptC-LptA copurification (15, 22). However, the results presented here suggest that structural features rather than specific amino acids residues are relevant to establish LptA-LptC interaction.

To gain further insights into this issue, we revisited the previously described conditional expression mutant ST-190 (24), in which a minitransposon (Tn*SS2*) with the arabinose-inducible *araBp* promoter oriented toward *lptAB* is inserted after nucleotide 413 of *lptC*, as assessed by sequencing of this region. We resequenced the right junction of the Tn*SS2* insertion and, while we confirmed our previous data (24), we also found that the minitransposon insertion had created an 8-nucleotide direct repeat of the target site after nucleotide 413 of *lptC* (within codon 138). In the resulting LptC mutant protein, the L138 residue was preserved and amino acids 139 to 191 were substituted by the transposon-encoded CLLIRSGHLGRIPGDPVID sequence (Fig. 1). Thus, this mutant expresses, from the major promoter of the *yrbG* operon, an *lptC* substitution allele (henceforth named *lptC190N*) which encodes the 1 to 138 N-terminal peptide of LptC fused to a 19-amino-acid-long C terminus encoded by the left end of the inserted minitransposon (Fig. 1). Therefore, the LptC truncation in ST-190 largely overlaps region 3 of the protein. The minitrans-

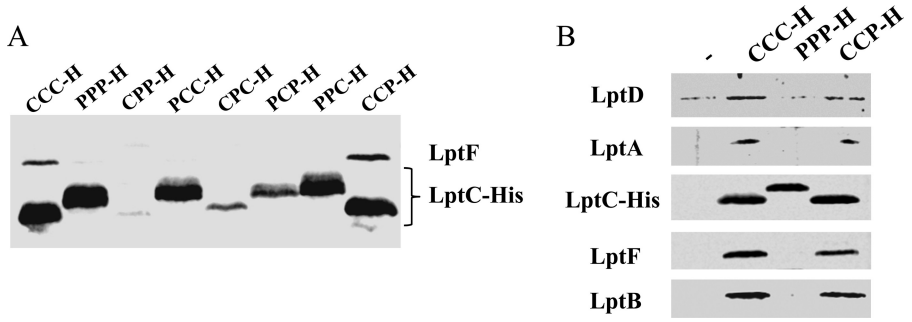

FIG 3 Assembly of the Lpt complex by *Pa*-LptC and LptC chimeras. Dodecyl β-D-maltoside-solubilized total membranes from AMM04 strains harboring pGS100 derivatives expressing the His-tagged proteins of interest were affinity purified using a Talon metal affinity resin, as described in Materials and Methods. Proteins were then fractionated by SDS-PAGE and immunoblotted with suitable antibodies to detect the corresponding proteins in the fraction. (A) Assembly of the Lpt IM complex. Samples were prepared from AMM04 harboring the pGS100 derivatives pGS108 (expressing *Ec*-LptC-H, CCC), pGS200 (expressing *Pa*-LptC-H, PPP), or those expressing His-tagged LptC chimeras, namely, pGS201H (CPP-H), pGS202H (PCC-H), pGS203H (CPC-H), pGS204H (PCP-H), pGS206H (CCP-H), and pGS207H (PPC-H). Immunoblotting was performed with anti-LptF and anti-His antibodies to detect LptF and the different His-tagged LptC forms, respectively, which display different electrophoretic mobility on SDS-PAGE. (B) Assembly of the transenvelope Lpt complex. Samples were prepared from AM604 harboring pGS108 (*Ec*-LptC-H, CCC), pGS200 (*Pa*-LptC-H, PPP), the His-tagged LptC CCP chimera (pGS206H), or pGS100 expressing the His tag (−) as a negative control. Immunoblotting was performed with the antibodies anti-His (to detect the different LptC forms) and anti-LptA, anti-LptB, anti-LptF, and anti-LptD.

poson insertion occurs immediately upstream of the minor promoters *lptAp1p2* located within *lptC* (35). In nonpermissive (no arabinose) conditions, expression of *lptAB* might be driven by these minor promoters only, whereas, in permissive conditions, the strong promoter *araBp* is also active. The viability of ST-190 in the presence of arabinose (24) indicates that, under such conditions, LptC190N is functional, whereas the nonviability of the mutant in nonpermissive condition suggests that *lptAB* expression is either lacking or insufficient. Here, we show (Fig. 4) that ST-190 viability in nonpermissive condition can be rescued not only by ectopic expression of *lptC* but also by a plasmid harboring *lptAB*. This indicates that, in this mutant strain (i) *lptAB* genes are indeed expressed from the minor promoters and their expression level is sufficient for viability in the presence of a wild-type LptC; (ii) the truncated *lptC190N* allele is defective when *lptAB* is expressed only from the ancillary promoters *lptAp1p2*; and (iii) a higher expression level of *lptAB* (from *araBp* in permissive conditions and/or from the complementing plasmid in the absence of arabinose) suppresses the *lptC190N* growth defect. It thus appears that the *lptAB* expression level from the ancillary *lptAp1p2* promoters is limiting for the truncated *lptC190N* allele and that the C-terminal 53 residues of LptC are dispensable at least under conditions of higher (nonlimiting) *lptAB* expression levels.

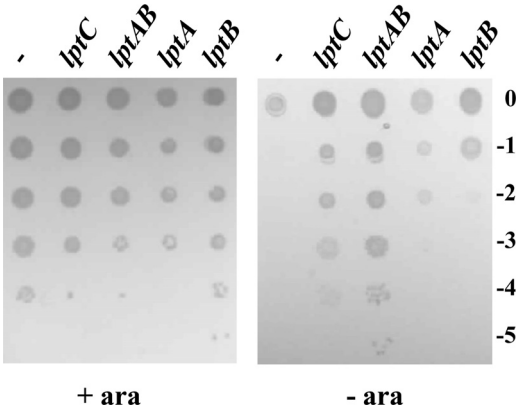

FIG 4 Growth of the ST-190 conditional expression mutant with different levels of LptA and/or LptB expression. Cultures of ST-190 transformed with pGS100 derivatives expressing the genes indicated on the top of each lane (*lptC* carried on pGS103; *lptAB* carried on pGS416; *lptA* carried on pGS321; *lptB* carried on pGS428) and grown in LD-chloramphenicol-arabinose were serially diluted 1:10 in microtiter wells and replica plated on agar plates supplemented (+ ara) or not supplemented (− ara) with arabinose. The log of the serial dilutions is indicated on the right of the panel.

To rule out that the observed phenotype depends on the ST-190 genetic background or the 19-amino-acid C-terminal substitution of the *lptC190N* allele, we tested whether plasmids expressing *lptC190N* or the truncated $lptC^{\Delta 139\text{-}191}$ allele either alone or coexpressed with *lptA*, *lptB*, or both could complement the conditional FL905 mutant. As shown in Table 3, neither *lptC190N* nor $lptC^{\Delta 139\text{-}191}$ complemented FL905 in the standard *lptC* complementation assay, whereas both mutants supported the growth of FL905 under nonpermissive conditions (no arabinose) when coexpressed with *lptAB*. Interestingly, whereas neither *lptC* mutant could complement when coexpressed with *lptA* only, coexpression of either *lptC190N* or $lptC^{\Delta 139\text{-}191}$ with *lptB* was able to rescue FL905 growth under nonpermissive conditions (Table 3). Thus, expression of *lptB* over the basal *lptAp1p2* level is required to suppress the *lptC190N* and $lptC^{\Delta 139\text{-}191}$ defects, whereas the expres-

TABLE 3 Complementation assays in LptC-depleted cells with additional ectopic expression[a] of *lptA-lptB*

Suppressing gene	Efficiency of plating with complementing *lptC* allele: None	*Ec-lptC*	*Ec-lptC190N*	*Ec-lptC*$^{\Delta 139\text{-}191}$	*Ec-lptC*^{G153R}	*Pa-lptC*
None	−	+	−	−	−	−
lptAB	−	+	+	+	−	±
lptA	−	+	−	−	−	−
lptB	−	+	+	+	−	+

[a] FL905 strains harboring pGS401 derivatives expressing different combinations of *lptC* complementing alleles and *lptA-lptB* suppressor genes were grown in LD with 0.2% arabinose and 25 μg/ml chloramphenicol. Serial dilutions in microtiter plates were replica plated on the same medium or without arabinose. Efficiency of plating in the nonpermissive condition (no arabinose) is expressed as follows: +, about 1; ±, between 10^{-2} and 10^{-3}; −, $<10^{-3}$.

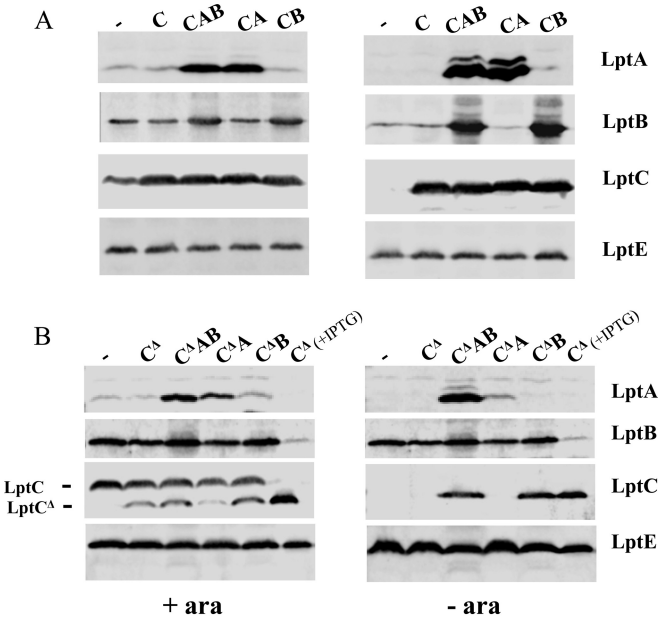

FIG 5 Expression levels of LptA, LptB, and LptC or LptC$^{\Delta 139\text{-}191}$ proteins in FL905 upon depletion of the chromosomally encoded LptC. FL905 cells transformed with pGS100 (−) or pGS100 derivatives harboring wild-type LptC (C, carried by pGS103) or LptC$^{\Delta 139\text{-}191}$ (C$^{\Delta}$, carried by pGS417) as indicated on the left of panels A and B, respectively, coexpressed with LptA (A, carried by pGS404 and pGS418, respectively), LptB (B, carried by pGS429 and pGS431, respectively), or LptAB (AB, carried by pGS415 and pGS419, respectively), as indicated on the top of the lanes, were grown in LD in the presence (+ ara) or absence (− ara) of arabinose and chloramphenicol, as described in Materials and Methods. Samples collected 4 h after a shift to the nonpermissive condition were analyzed by Western blotting using anti-LptA, anti-LptB, anti-LptC, and anti-LptE antibodies. An equal amount of cells (OD_{600}, 0.6) was loaded onto each lane. The migrations of full-length LptC and LptC$^{\Delta}$ are indicated on the left side of panel B. The last lane of each image in panel B (C$^{\Delta}$ + IPTG) was loaded with 10 μl of cell extract of FL905 harboring pGS417 (LptC$^{\Delta 139\text{-}191}$) arabinose depleted for 3 h and further incubated 1 h with 0.1 mM IPTG to induce expression of the truncated LptC protein. LptE level was used as a sample loading control.

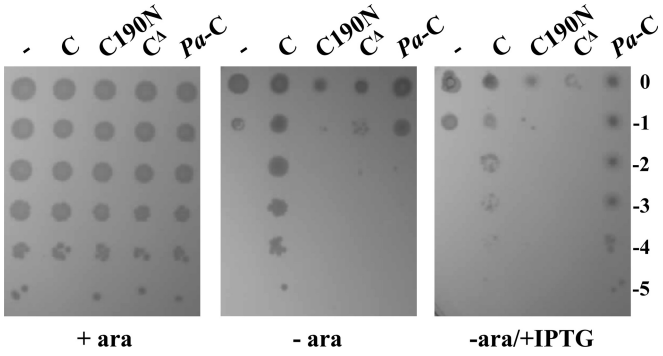

FIG 6 Rescue of FL905 growth by overexpression of truncated *Ec-lptC* or *Pa-lptC* alleles. FL905 cells transformed with pGS100 (−) or pGS100 derivatives harboring wild-type LptC (pGS103), LptC$^{\Delta 139\text{-}191}$ (pGS417), LptC190N (pGS408), or *Pa*-LptC (pGS111), as indicated on top of the lanes, were grown in LD-chloramphenicol-arabinose, serially diluted 1:10 in microtiter wells, and replica plated on LD-agar plates with chloramphenicol and with (+ ara) or without (− ara) arabinose and with IPTG (+ IPTG) to induce the *lptC* allele on the plasmids, as described in Materials and Methods. The log of the serial dilutions is indicated on the right.

sion level of *lptA* does not seem to be a limiting factor. As in ST-190 (carrying the *lptC190N* allele), growth under nonpermissive conditions requires both *lptA* and *lptB* overexpression; we speculate that, in this mutant strain, the minitransposon insertion in close proximity to *lptAp1p2* and/or the different genetic background might negatively affect the expression of the downstream *lptAB* operon. On the contrary, the defective *lptC*^{G153R} mutation was not suppressed by increased *lptB* and/or *lptAB* expression (Table 3).

LptB is a limiting factor for stabilization of LptC$^{\Delta 139\text{-}191}$. Suppression of LptC defects by increased expression of LptB is intriguing, as it reveals functional interactions between the cytoplasmic LptB and the bitopic IM LptC protein. LptB has been implicated not only in providing energy through ATP hydrolysis but also in the assembly of the IM complex (10). It could be hypothesized that the assembly of LptC lacking the C-terminal domain is partially defective, thus leading to LptC instability, and that a level of LptB higher than that provided by the ancillary promoters *lptAp1* and *lptAp2* is necessary for C-terminally truncated LptC assembly and stability. We therefore examined the levels of C-terminally truncated LptC with *lptB* expressed from a plasmid. FL905 cells coexpressing wild-type *lptC* or *lptC*$^{\Delta 139\text{-}191}$ with *lptA*, *lptB*, or *lptAB* were grown up to the exponential phase and shifted into a medium lacking arabinose to deplete the chromosomally encoded wild-type LptC while allowing expression of the alleles from the complementing plasmids. Samples were then taken from cultures grown in the presence or in the absence of arabinose 240 min after the shift to nonpermissive conditions and analyzed by Western blotting using anti-LptA, anti-LptC, and anti-LptB antibodies. The level of the LptE protein was used as a sample loading control. As shown in Fig. 5, the expression level of LptC$^{\Delta 139\text{-}191}$ in depleted FL905 cells was detectable when *lptAB* or *lptB* alone was also ectopically expressed, whereas it was not when the *lptAB* operon was expressed from the minor chromosomal promoters only. Interestingly, in the *lptC*$^{\Delta 139\text{-}191}$ mutant background, the LptA level also increased when *lptA* was coexpressed with *lptB* (Fig. 5B, compare lanes LptC$^{\Delta 139\text{-}191}$ LptAB and LptC$^{\Delta 139\text{-}191}$ LptA), in keeping with our previous observations (15) that the increased amount of wild-type or truncated LptC helps in stabilizing LptA.

The above data suggest that a higher level of *lptB* expression mediates stabilization of LptC$^{\Delta 139\text{-}191}$, thus suppressing the lethal phenotype of FL905 cells carrying the truncated *lptC* allele. However, neither LptC$^{\Delta 139\text{-}191}$ nor LptC190N overexpressed from an IPTG-inducible promoter were able to rescue growth of FL905 cells under nonpermissive conditions (Fig. 6), thus confirming that an increased level of LptB is able to stabilize the otherwise unstable LptC truncated proteins. In line with these data is the finding that His-tagged truncated *Ec*-LptC protein missing region 3 (CCΔ) is not detectable when *lptB* is not overexpressed (see panel E in Fig. S4 in the supplemental material); moreover, this truncated form of LptC appears to be highly toxic when expressed from an IPTG-inducible promoter (see panel D in Fig. S4).

Overexpression of *lptB* rescues LptC-depleted cells complemented by *Pa-lptC*. We showed (Fig. 2) that expression of the highly divergent *Pa-lptC* gene from a plasmid did not complement FL905 for growth in the absence of arabinose. To assess whether *lptB* expression could be a limiting factor for complementation by the xenogeneic *Pa*-LptC, we tested whether increased expression

of *lptB* could rescue growth of *Ec*-LptC-depleted cells. FL905 cells were transformed with plasmids coexpressing *Pa-lptC* with *lptA*, *lptB*, or *lptAB* from *E. coli*. As shown in Table 3, ectopic expression of *lptB* rescued growth of FL905 complemented by *Pa-lptC*. However, overexpression of *Pa-lptC* with (see Fig. S2 in the supplemental material) and without (Fig. 6) the His tag from an IPTG-inducible promoter also rescued FL905 growth, thus supporting the view that Pa-LptC might have a lower affinity for the *E. coli* IM Lpt complex. Although His-tagged Pa-LptC is able to complement the FL905 growth defect, the level of His-tagged Pa-LptC is very low and not detectable with anti-His antibodies (see Fig. S4). Overall, these data confirm that *P. aeruginosa* open reading frame PA4459 encodes the functional homologue of *E. coli* LptC.

LptB mutants in either ATPase or assembly function do not suppress the growth defect of C-terminally deleted LptC. The ATPase activity of LptB can be genetically separated from its ability to assemble the IM LptBCFG complex (10). Indeed, $LptB^{E163Q}$ mutant is catalytically inactive but retains the ability to interact with the transmembrane regions of LptFG. On the contrary, LptB F90Y and F90A amino acid substitutions do not affect LptB ATPase activity, although they impair to different extents the LptB assembly properties (10). We therefore tested whether ectopic expression of *lptB* mutants E163Q, F90Y, and F90A suppresses lethality of the truncated $lptC^{\Delta 139\text{-}191}$ allele. It should be remembered that, in our experimental setting, a wild-type copy of *lptB* is expressed from the ancillary *lptAp1p2* chromosomal promoters. None of the coexpressed *lptB* mutants affected the growth of FL905 complemented by wild-type *lptC* (Fig. 7). On the contrary, ectopic expression of $LptB^{E163Q}$ and $LptB^{F90A}$ did not rescue the growth of FL905 complemented by $LptC^{\Delta 139\text{-}191}$, whereas the partial loss of function mutant $LptB^{F90Y}$ was able to suppress the $LptC^{\Delta 139\text{-}191}$ growth defect (Fig. 7).

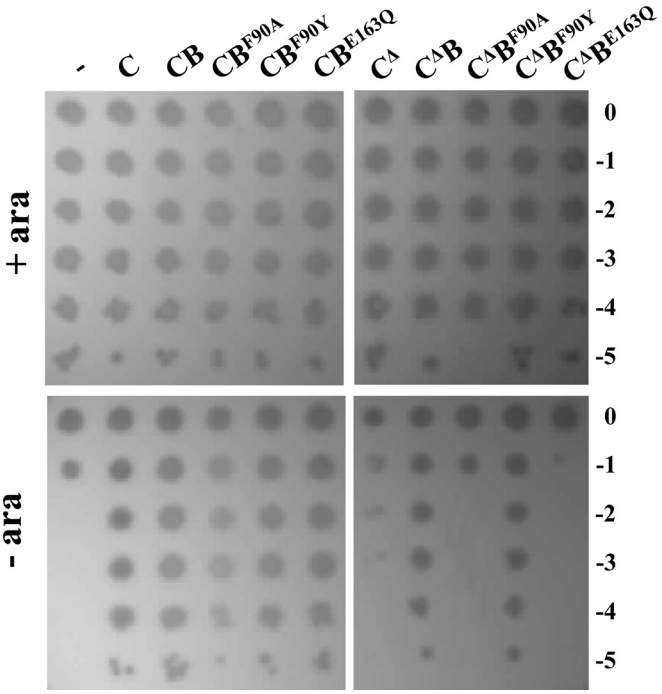

FIG 7 Suppression of LptC defects by *lptB* mutants. FL905 cells transformed with pGS100 (−) or pGS100 derivatives harboring wild-type LptC (C, carried by pGS103) or $LptC^{\Delta 139\text{-}191}$ (C^{Δ}, pGS417) coexpressed with LptB (B, carried by pGS429 and pGS431, respectively), $LptB^{F90A}$ (B^{F90A} carried by pGS429-$LptB^{F90A}$ and pGS431-$LptB^{F90A}$, respectively), $LptB^{F90Y}$ (B^{F90Y}, carried by pGS429-$LptB^{F90Y}$ and pGS431-$LptB^{F90Y}$, respectively), or $LptB^{E163Q}$ (B^{E163Q}, carried by pGS429-$LptB^{E163Q}$ and pGS431-$LptB^{E163Q}$, respectively), as indicated on top of the lanes, were grown in LD-chloramphenicol-arabinose, serially diluted 1:10 in microtiter wells, and replica plated on LD-agar plates with chloramphenicol in the presence (+ ara) or in the absence (− ara) of arabinose, as described in Materials and Methods. The log of the serial dilutions is indicated on the right.

DISCUSSION

LptC is an unusual component of the IM $LptB_2FG$ complex, an atypical ABC exporter (36) that energizes LPS transport. LptC role in LPS transport is not completely understood. Its transmembrane N-terminal domain is dispensable, whereas the soluble periplasmic domain interacts with both LptA and the IM $LptB_2FG$ complex via the C- and N-terminal regions, respectively (16, 22). LptC is thought to bind LPS and to transfer it to LptA in an energy-dependent way (9, 17), although its association with $LptB_2FG$ does not affect LptB ATPase activity (8). Here, we have further dissected the LptC functional domains by analyzing the properties of LptC C-terminal deletions and of *Pa*-LptC and *Ec*-/*Pa*-LptC chimeras in *E. coli*.

The LptC C-terminal region can be replaced by a xenogeneic divergent sequence. Among the seven components of the Lpt machinery, *Pa*-LptC is the most divergent from the *E. coli* homologue (19% amino acid sequence identity) and does not seem to bear the most conserved of three motifs (encompassing amino acids 94 to 143) identified in LptC on the basis of sequence alignments of a panel of homologues (Fig. 1; see also Fig. S1 in the supplemental material).

Ectopic expression of *Pa*-LptC, unlike *Ec*-LptC expression, does not complement *Ec*-LptC-depleted *E. coli* mutants in the reference *lptC* complementation test. We exploited these noncomplementing conditions to dissect *Pa*-LptC and implicate specific regions in this phenotype. The *Pa*-LptC protein appears to be defective in the assembly with the *E. coli* components of the Lpt multiprotein machinery, as it does not interact with the *Ec*-$LptB_2FG$ IM subcomplex (Fig. 3); as previously shown, such interaction is necessary *in vivo* for LptA recruitment and for the whole Lpt complex assembly (22). On the other hand, overexpression of *Pa*-LptC by IPTG induction complements FL905 for growth in nonpermissive conditions, thus suggesting that a viable amount of hybrid Lpt machine can be assembled and that the inefficient interactions of *Pa*-LptC with the *Ec*-Lpt proteins may be overcome by *Pa*-LptC overexpression (Fig. 6).

Analysis of *Ec*-/*Pa*-LptC chimeras, in which the three LptC regions from the two organisms were swapped in all possible combinations, indicates that the *E. coli* LptC protein tolerates the substitution of the C-terminal region with the corresponding *P. aeruginosa* homologous region. Indeed, the LptC CCP chimera complements LptC-depleted *E. coli* in the *lptC* complementation test (Fig. 2) and assembles the LptC complex (Fig. 3B), whereas the noncomplementing *Ec*-/*Pa*-LptC chimeras, like *Pa*-LptC, are unable to bind the IM $LptB_2FG$ subcomplex *in vivo*. Based on these data, it appears that regions 1 and 2 are relevant for LptC function and Lpt complex assembly, as their substitutions with xenogeneic divergent sequences is not tolerated, whereas the C-terminal region 3 may have an ancillary role. As discussed below, it is possible that the presence of a structured C-terminal domain from *P. aeruginosa* helps to stabilize the CCP chimera.

Functional interaction between LptB and LptC. The C-terminal region of LptC has been previously implicated in binding to LptA. Indeed, the unviable LptC^{G153R} mutant fails to interact with LptA and to assemble the transenvelope complex, although it associates with the IM LptB$_2$FG subcomplex (15, 22). Moreover, by *in vivo* photo-cross-linking, the C-terminal LptC residues A172 and Y182 have been implicated in binding LptA (16). These three residues, therefore, define the LptA-LptC interaction interface.

In contrast, we show here not only that the substitution of the C-terminal region with the highly divergent *P. aeruginosa* homologous region is viable but also that *lptC* alleles that are either C-terminally truncated or substituted by an unrelated sequence (*lptC*$^{\Delta 139\text{-}191}$ and *lptC190N*, respectively) and the highly divergent *Pa-lptC* homologue, although unable to complement in the reference *lptC* complementation test, are viable under conditions of nonlimiting expression of *lptB*. Thus, a higher expression of *lptB* suppresses the growth defect of these *lptC* alleles. This suggests that, upon repression of chromosomal *araBp-lptC*, *lptA* expression from *lptAp1p2* promoters is sufficient for growth, whereas *lptB* expression is the limiting factor for viability of *lptC*$^{\Delta 139\text{-}191}$, *lptC190N*, or *Pa-lptC*-complemented *E. coli*.

LptC$^{\Delta 139\text{-}191}$ stabilization appears crucial for FL905 viability upon LptC depletion. Indeed, the LptC$^{\Delta 139\text{-}191}$ steady-state level increases when *lptB* but not *lptA* is overexpressed (Fig. 5). Interestingly, LptC$^{\Delta 139\text{-}191}$ stabilization by increased expression of *lptB* seems also to positively affect LptA abundance (Fig. 5), thus implicating LptB in the control of LptC-LptA interactions. The tight genetic association of *lptCAB*, which belong to the same *yrbG* operon (24), and the presence of two ancillary promoters within *lptC* for the nested *lptAB* operon (4, 35) may be instrumental in maintaining balanced expression levels of the three encoded proteins.

The finding that ectopic expression of *lptB* allows functioning of mutant LptC or *P. aeruginosa-E. coli* hybrid Lpt machineries raises questions on the functional interactions between LptC and LptB. LptB is the IM-associated ATPase that interacts with the IM complex and provides the energy required for LPS transport (8, 9). LptB plays also a role in the assembly of the IM LptB$_2$FGC subcomplex and, interestingly, these two functions can be genetically separated (10). In fact, the LptB^{E163Q} mutant is catalytically inactive but retains the ability to interact with the transmembrane regions of LptFG. On the contrary, the F90A and F90Y amino acid substitutions do not affect LptB ATPase activity but impair, the former completely, the latter only partially, LptB assembly properties. We found that ectopic expression of both the catalytically inactive LptB^{E163Q} and assembly-defective LptB^{F90A} mutants (10) does not rescue the lethal phenotype of FL905 cells complemented by *lptC*$^{\Delta 139\text{-}191}$, whereas LptB^{F90Y} does. It should be remembered that, although partially defective in the LptCFG complex assembly, LptB^{F90Y} is able to complement a *lptB*-deficient mutant (10); therefore, our results show that a nonlimiting expression of LptB endowed with both ATPase and assembly functions is required for the suppression of the lethal phenotype of C-terminally truncated LptC.

The role of LptB in the assembly of the Lpt machine (10) may explain why the level of LptB expression may be a limiting factor in the presence of the C-terminally truncated LptC. In fact, such LptC mutant, although fully proficient for interaction with LptB$_2$FG, is highly unstable and may cause a rapid functional inactivation of the IM Lpt subcomplex, therefore affecting the recruitment of LptA and of the OM LptDE subcomplex. In LptC-depleted cells complemented by wild-type LptC, the expression level of *lptB* from the ancillary promoters may be sufficient for the assembly of an adequate number of stable Lpt IM subcomplexes. On the contrary, the rapid inactivation of IM subcomplexes containing C-terminally truncated LptC would result in a higher turnover of such Lpt IM subcomplexes, and thus, an increased amount of LptB would be required to assemble new functional IM subcomplexes sufficient for cell growth.

Interestingly, growth of LptC-depleted *E. coli* cells complemented by *Pa*-LptC can be rescued by both ectopic *lptB* expression and overexpression of *Pa-lptC* from an inducible IPTG promoter, whereas overexpression of *E. coli* C-terminally truncated or substituted *lptC* alleles does not. These data suggest that, in this case, the limiting factor, rather than *Pa*-LptC stability, is a lower affinity of the *P. aeruginosa* component for *E. coli* LptFG (Fig. 3A) and that the amount of IM subcomplexes sufficient to support growth could be achieved by increasing the level of either *Pa*-LptC or *Ec*-LptB. These findings are in agreement with a previous work showing that LptH (the *P. aeruginosa* LptA homologue) can replace *Ec*-LptA (19) when a functional IM LptCB$_2$FG complex is in place to recruit LptA/LptH and, therefore, the OM LptDE subcomplex. Overall, the results here reported reinforce the view that the assembly of the IM complex is a control step for the formation of a functional transenvelope bridge.

On the other hand, the defective *lptC*^{G153R} mutation was not suppressed by increased *lptB* expression. LptC^{G153R} is a loss-of-function mutant protein able to assemble the IM LptB$_2$FG complex but unable to interact with LptA (15, 22). As judged by its crystal structure, the LptC^{G153R} protein maintains the overall β-jellyroll fold, and we proposed that the protein can be defective either in a conformational change required for LptA interaction or in LPS binding (22); likely, none of these defects can be suppressed by increased LptB levels.

What is the role of LptC in LPS transport? The current model for LPS export postulates that LPS in the outer leaflet of the IM is extracted by the LptCFG complex with energy provided by the associated LptB ATPase component (9, 10). LptC cannot extract LPS on its own, but LPS likely is delivered to LptC by LptF or LptG or by both. LptC, which is functional even without its transmembrane domain (22), binds LPS at the N-terminal region (via residue T47) and transfers it to LptA, and both steps require ATP hydrolysis (9). LptA is thought to interact with the N-terminal region of LptD and to deliver the LPS to the LptDE translocon for assembly at the OM (12, 16, 20). The Lpt fold that is shared by LptA, LptC, and LptD (12, 17, 18, 20) and predicted in the periplasmic region of LptF and LptG (15, 22) appears to be a key element in driving the assembly of the transenvelope bridge. It has been suggested that these proteins may form a hydrophobic groove that accommodates the lipid moiety of LPS for its transport from the inner membrane to the outer membrane (9, 16).

Here, we show that LPS transport can be accomplished by Lpt machines carrying either C-terminally truncated LptC proteins or the highly divergent Pa-LptC (under specific conditions, i.e., increased *lptB* level and/or *Pa-lptC* overexpression) or the chimeric CCP LptC protein in which the C terminus is derived from *P. aeruginosa*. Since the CCP chimera appears fully functional, we speculate that the C-terminal region of Pa-LptC can fully substitute the corresponding region in *Ec*-LptC in recruiting *Ec*-LptA and building the hydrophobic groove for LPS export. Similarly,

we propose that *Pa*-LptC is not defective in LptA recruitment and that its inability to assemble a functional Lpt machine relies on its low affinity to the IM $LptB_2FG$ complex. Such a defect is suppressed either by an increased level of LptB or by Pa-LptC overexpression, which helps stabilize the IM *Pa*-LptC/*Ec*-$LptB_2FG$ hybrid subcomplex and, as a consequence, allows the recruitment of *Ec*-LptA. The functional interaction between LptC and LptB is in line with a regulatory role of LptC in modulating the Lpt protein bridge formation (22) and/or the activity of the IM $LptB_2FG$ complex (37) It is not clear at the structural level how a C-terminally truncated LptC may function in recruiting LptA and assembling a functional Lpt machine. Based on structure prediction (see Fig. S2 in the supplemental material), the C-terminally truncated LptC protein seems to maintain the β-jellyroll structure; therefore, the binding between the C-terminally truncated LptC and LptA might occur through the edge of their respective β jellyroll, thus allowing the assembly of a functional Lpt machine.

Interestingly, deletions of the C-terminal regions of LptC seem to be tolerated also by species other than *E. coli*, as witnessed by the isolation of transposon insertion mutants in the C-terminal region of LptC in *P. aeruginosa* (http://ausubellab.mgh.harvard.edu) (Fig. 1) and *Ralstonia solanacearum* (38) and of an *lptC* frameshift mutation after codon 134 in *Salmonella enterica* conferring bile resistance (39).

It will be crucial to understand which are the structural bases for the functioning of Lpt machineries carrying truncated LptC proteins. Despite extensive studies on the Lpt machinery, we still lack structural data on the LptFG IM components and on LptC-LptA and LptC-LptFG interactions, which are fundamental to understand at the molecular level the functioning of LPS export machinery.

ACKNOWLEDGMENTS

We thank Daniel Khane and Natividad Ruiz for providing antibodies against LptE and LptB, respectively.

This research was supported in part by Fondazione Fibrosi Cistica, grant FFC13/2010 (*Pseudomonas aeruginosa* lipopolysaccharide cell surface transport is a target process for developing new antimicrobials), by MIUR Regione Lombardia, project 30190679 (Nuovi antibiotici mediante rational design), by MIUR PRIN 2012WJSX8K (Host-microbe interaction models in mucosal infections: development of novel therapeutic strategies), and by Fondazione Cariplo grant 2010.0653 (Outer membrane biogenesis in Gram-negative bacteria as a target for innovative antibacterial drugs).

FUNDING INFORMATION

This work, including the efforts of Alessandra Polissi, was funded by Fondazione Fibrosi Cistica (FFC13/2010). This work, including the efforts of Alessandra Polissi, was funded by MIUR Regione Lombardia (30190679). This work, including the efforts of Alessandra Polissi, was funded by MIUR PRIN (2012WJSX8K). This work, including the efforts of Paola Sperandeo, was funded by Fondazione Cariplo (Cariplo Foundation) (2010.0653).

REFERENCES

1. **Silhavy TJ, Kahne D, Walker S.** 2010. The bacterial cell envelope. Cold Spring Harb Perspect Biol **2:**a000414.
2. **Nikaido H.** 2003. Molecular basis of bacterial outer membrane permeability revisited. Microbiol Mol Biol Rev **67:**593–656. http://dx.doi.org/10.1128/MMBR.67.4.593-656.2003.
3. **Wu T, McCandlish AC, Gronenberg LS, Chng SS, Silhavy TJ, Kahne D.** 2006. Identification of a protein complex that assembles lipopolysaccharide in the outer membrane of *Escherichia coli*. Proc Natl Acad Sci U S A **103:**11754–11759. http://dx.doi.org/10.1073/pnas.0604744103.
4. **Sperandeo P, Cescutti R, Villa R, Di Benedetto C, Candia D, Dehò G, Polissi A.** 2007. Characterization of *lptA* and *lptB*, two essential genes implicated in lipopolysaccharide transport to the outer membrane of *Escherichia coli*. J Bacteriol **189:**244–253. http://dx.doi.org/10.1128/JB.01126-06.
5. **Sperandeo P, Lau FK, Carpentieri A, De Castro C, Molinaro A, Dehò G, Silhavy TJ, Polissi A.** 2008. Functional analysis of the protein machinery required for transport of lipopolysaccharide to the outer membrane of *Escherichia coli*. J Bacteriol **190:**4460–4469. http://dx.doi.org/10.1128/JB.00270-08.
6. **Ruiz N, Gronenberg LS, Kahne D, Silhavy TJ.** 2008. Identification of two inner membrane proteins required for the transport of lipopolysaccharide to the outer membrane of *Escherichia coli*. Proc Natl Acad Sci U S A **105:**5537–5542. http://dx.doi.org/10.1073/pnas.0801196105.
7. **Chng SS, Gronenberg LS, Kahne D.** 2010. Proteins required for lipopolysaccharide assembly in *Escherichia coli* form a transenvelope complex. Biochemistry **49:**4565–4567. http://dx.doi.org/10.1021/bi100493e.
8. **Narita S, Tokuda H.** 2009. Biochemical characterization of an ABC transporter LptBFGC complex required for the outer membrane sorting of lipopolysaccharides. FEBS Lett **583:**2160–2164. http://dx.doi.org/10.1016/j.febslet.2009.05.051.
9. **Okuda S, Freinkman E, Kahne D.** 2012. Cytoplasmic ATP hydrolysis powers transport of lipopolysaccharide across the periplasm in *E. coli*. Science **338:**1214–1217. http://dx.doi.org/10.1126/science.1228984.
10. **Sherman DJ, Lazarus MB, Murphy L, Liu C, Walker S, Ruiz N, Kahne D.** 2014. Decoupling catalytic activity from biological function of the ATPase that powers lipopolysaccharide transport. Proc Natl Acad Sci U S A **111:**4982–4987. http://dx.doi.org/10.1073/pnas.1323516111.
11. **Freinkman E, Chng SS, Kahne D.** 2011. The complex that inserts lipopolysaccharide into the bacterial outer membrane forms a two-protein plug-and-barrel. Proc Natl Acad Sci U S A **108:**2486–2491. http://dx.doi.org/10.1073/pnas.1015617108.
12. **Qiao S, Luo Q, Zhao Y, Zhang XC, Huang Y.** 2014. Structural basis for lipopolysaccharide insertion in the bacterial outer membrane. Nature **511:**108–111. http://dx.doi.org/10.1038/nature13484.
13. **Chng SS, Ruiz N, Chimalakonda G, Silhavy TJ, Kahne D.** 2010. Characterization of the two-protein complex in *Escherichia coli* responsible for lipopolysaccharide assembly at the outer membrane. Proc Natl Acad Sci U S A **107:**5363–5368. http://dx.doi.org/10.1073/pnas.0912872107.
14. **Chimalakonda G, Ruiz N, Chng SS, Garner RA, Kahne D, Silhavy TJ.** 2011. Lipoprotein LptE is required for the assembly of LptD by the beta-barrel assembly machine in the outer membrane of *Escherichia coli*. Proc Natl Acad Sci U S A **108:**2492–2497. http://dx.doi.org/10.1073/pnas.1019089108.
15. **Sperandeo P, Villa R, Martorana AM, Samalikova M, Grandori R, Dehò G, Polissi A.** 2011. New insights into the Lpt machinery for lipopolysaccharide transport to the cell surface: LptA-LptC interaction and LptA stability as sensors of a properly assembled transenvelope complex. J Bacteriol **193:**1042–1053. http://dx.doi.org/10.1128/JB.01037-10.
16. **Freinkman E, Okuda S, Ruiz N, Kahne D.** 2012. Regulated assembly of the transenvelope protein complex required for lipopolysaccharide export. Biochemistry **51:**4800–4806. http://dx.doi.org/10.1021/bi300592c.
17. **Tran AX, Dong C, Whitfield C.** 2010. Structure and functional analysis of LptC, a conserved membrane protein involved in the lipopolysaccharide export pathway in *Escherichia coli*. J Biol Chem **285:**33529–33539. http://dx.doi.org/10.1074/jbc.M110.144709.
18. **Suits MD, Sperandeo P, Dehò G, Polissi A, Jia Z.** 2008. Novel structure of the conserved Gram-negative lipopolysaccharide transport protein A and mutagenesis analysis. J Mol Biol **380:**476–488. http://dx.doi.org/10.1016/j.jmb.2008.04.045.
19. **Bollati M, Villa R, Gourlay LJ, Benedet M, Dehò G, Polissi A, Barbiroli A, Martorana AM, Sperandeo P, Bolognesi M, Nardini M.** 2015. Crystal structure of LptH, the periplasmic component of the lipopolysaccharide transport machinery from *Pseudomonas aeruginosa*. FEBS J **282:**1980–1997. http://dx.doi.org/10.1111/febs.13254.
20. **Dong H, Xiang Q, Gu Y, Wang Z, Paterson NG, Stansfeld PJ, He C, Zhang Y, Wang W, Dong C.** 2014. Structural basis for outer membrane lipopolysaccharide insertion. Nature **511:**52–56. http://dx.doi.org/10.1038/nature13464.
21. **Wang Z, Xiang Q, Zhu X, Dong H, He C, Wang H, Zhang Y, Wang W, Dong C.** 2014. Structural and functional studies of conserved

nucleotide-binding protein LptB in lipopolysaccharide transport. Biochem Biophys Res Commun **452:**443–449. http://dx.doi.org/10.1016/j.bbrc.2014.08.094.

22. **Villa R, Martorana AM, Okuda S, Gourlay LJ, Nardini M, Sperandeo P, Dehò G, Bolognesi M, Kahne D, Polissi A.** 2013. The *Escherichia coli* Lpt transenvelope protein complex for lipopolysaccharide export is assembled via conserved structurally homologous domains. J Bacteriol **195:**1100–1108. http://dx.doi.org/10.1128/JB.02057-12.
23. **Narita S, Masui C, Suzuki T, Dohmae N, Akiyama Y.** 2013. Protease homolog BepA (YfgC) promotes assembly and degradation of beta-barrel membrane proteins in *Escherichia coli*. Proc Natl Acad Sci U S A **110:**E3612–E3621. http://dx.doi.org/10.1073/pnas.1312012110.
24. **Serina S, Nozza F, Nicastro G, Faggioni F, Mottl H, Dehò G, Polissi A.** 2004. Scanning the *Escherichia coli* chromosome by random transposon mutagenesis and multiple phenotypic screening. Res Microbiol **155:**692–701. http://dx.doi.org/10.1016/j.resmic.2004.05.006.
25. **Stover CK, Pham XQ, Erwin AL, Mizoguchi SD, Warrener P, Hickey MJ, Brinkman FS, Hufnagle WO, Kowalik DJ, Lagrou M, Garber RL, Goltry L, Tolentino E, Westbrock-Wadman S, Yuan Y, Brody LL, Coulter SN, Folger KR, Kas A, Larbig K, Lim R, Smith K, Spencer D, Wong GK, Wu Z, Paulsen IT, Reizer J, Saier MH, Hancock RE, Lory S, Olson MV.** 2000. Complete genome sequence of *Pseudomonas aeruginosa* PAO1, an opportunistic pathogen. Nature **406:**959–964. http://dx.doi.org/10.1038/35023079.
26. **Li XM, Shapiro LJ.** 1993. Three-step PCR mutagenesis for linker scanning. Nucleic Acids Res **21:**3745–3748. http://dx.doi.org/10.1093/nar/21.16.3745.
27. **Ghisotti D, Chiaramonte R, Forti F, Zangrossi S, Sironi G, Dehò G.** 1992. Genetic analysis of the immunity region of phage-plasmid P4. Mol Microbiol **6:**3405–3413. http://dx.doi.org/10.1111/j.1365-2958.1992.tb02208.x.
28. **Bailey TL, Elkan C.** 1994. Fitting a mixture model by expectation maximization to discover motifs in biopolymers. Proc Int Conf Intell Syst Mol Biol **2:**28–36.
29. **Bailey TL, Boden M, Buske FA, Frith M, Grant CE, Clementi L, Ren J, Li WW, Noble WS.** 2009. MEME suite: tools for motif discovery and searching. Nucleic Acids Res **37:**W202-208. http://dx.doi.org/10.1093/nar/gkp335.
30. **Corpet F.** 1988. Multiple sequence alignment with hierarchical clustering. Nucleic Acids Res **16:**10881–10890. http://dx.doi.org/10.1093/nar/16.22.10881.
31. **Henikoff S, Henikoff JG.** 1992. Amino acid substitution matrices from protein blocks. Proc Natl Acad Sci U S A **89:**10915–10919. http://dx.doi.org/10.1073/pnas.89.22.10915.
32. **Williams KP, Gillespie JJ, Sobral BW, Nordberg EK, Snyder EE, Shallom JM, Dickerman AW.** 2010. Phylogeny of *Gammaproteobacteria*. J Bacteriol **192:**2305–2314. http://dx.doi.org/10.1128/JB.01480-09.
33. **Yang J, Yan R, Roy A, Xu D, Poisson J, Zhang Y.** 2015. The I-TASSER suite: protein structure and function prediction. Nat Methods **12:**7–8.
34. **Punta M, Simon I, Dosztanyi Z.** 2015. Prediction and analysis of intrinsically disordered proteins. Methods Mol Biol **1261:**35–59. http://dx.doi.org/10.1007/978-1-4939-2230-7_3.
35. **Martorana AM, Sperandeo P, Polissi A, Dehò G.** 2011. Complex transcriptional organization regulates an *Escherichia coli* locus implicated in lipopolysaccharide biogenesis. Res Microbiol **162:**470–482. http://dx.doi.org/10.1016/j.resmic.2011.03.007.
36. **Davidson AL, Dassa E, Orelle C, Chen J.** 2008. Structure, function, and evolution of bacterial ATP-binding cassette systems. Microbiol Mol Biol Rev **72:**317–364. http://dx.doi.org/10.1128/MMBR.00031-07.
37. **Okuda S, Sherman DJ, Silhavy TJ, Ruiz N, Kahne D.** 2016. Lipopolysaccharide transport and assembly at the outer membrane: the PEZ model. Nat Rev Microbiol **14:**337–345. http://dx.doi.org/10.1038/nrmicro.2016.25..
38. **Yang WC, Lin YM, Cheng YS, Cheng CP.** 2013. Ralstonia solanacearum RSc0411 (lptC) is a determinant for full virulence and has a strain-specific novel function in the T3SS activity. Microbiology **159:**1136–1148. http://dx.doi.org/10.1099/mic.0.064915-0.
39. **Hernández SB, Cota I, Ducret A, Aussel L, Casadesus J.** 2012. Adaptation and preadaptation of *Salmonella enterica* to bile. PLoS Genet **8:**e1002459. http://dx.doi.org/10.1371/journal.pgen.1002459.
40. **Hanahan D.** 1983. Studies on transformation of *Escherichia coli* with plasmids. J Mol Biol **166:**557–580. http://dx.doi.org/10.1016/S0022-2836(83)80284-8.
41. **Grant SG, Jessee J, Bloom FR, Hanahan D.** 1990. Differential plasmid rescue from transgenic mouse DNAs into *Escherichia coli* methylation-restriction mutants. Proc Natl Acad Sci U S A **87:**4645–4649. http://dx.doi.org/10.1073/pnas.87.12.4645.
42. **Casadaban MJ.** 1976. Transposition and fusion of the *lac* genes to selected promoters in *Escherichia coli* using bacteriophage lambda and mu. J Mol Biol **104:**541–555. http://dx.doi.org/10.1016/0022-2836(76)90119-4.
43. **Bachmann BJ.** 1987. Derivatives and genotypes of some mutant derivatives of *Escherichia coli* K-12, p 1191–1219. *In* Ingraham JL, Low KB, Magasanik B, Schaechter M, Umbarger HE (ed), *Escherichia coli* and *Salmonella* Typhimurium cellular and molecular biology, vol 2. ASM Press, Washington, DC.
44. **Sperandeo P, Pozzi C, Dehò G, Polissi A.** 2006. Nonessential KDO biosynthesis and new essential cell envelope biogenesis genes in the *Escherichia coli yrbG-yhbG* locus. Res Microbiol **157:**547–558. http://dx.doi.org/10.1016/j.resmic.2005.11.014.